Orthogonal effect of exchange and correlation parameters in density functional theory to compute geometric and spectroscopic quantities.

Aurélien Moncomble, Jean-Paul Cornard

Received: 31 December 2023 | Revised: 26 March 2024 | Accepted: 3 April 2024

DOI: 10.1002/jcc.27382

RESEARCH ARTICLE

Journal of COMPUTATIONAL CHEMISTRY WILEY

Orthogonal effect of exchange and correlation parameters in density functional theory to compute geometric and spectroscopic quantities

Aurélien Moncomble | Jean-Paul Cornard

Laboratoire de Spectroscopie pour les Interactions, la Réactivité et l'Environnement, Université Lille, CNRS, UMR 8516, LASIRE, Lille, France

Correspondence
Aurélien Moncomble, Laboratoire de Spectroscopie pour les Interactions, la Réactivité et l'Environnement, Université Lille, CNRS, UMR 8516, LASIRE F-59000 Lille, France.
Email: aurelien.moncomble@univ-lille.fr

Funding information
Centre National de la Recherche Scientifique; Université de Lille

Abstract

The influence of the composition of the functional used for density functional theory computations on one structural parameter (a dihedral angle) and a spectroscopic parameter (absorption wavelength) is assessed in this study on the basis of two molecules (flavonols). In this kind of molecules, these two parameters should be correlated according to the nature of the electronic transition involved. However, it is shown herein that by varying the proportion of true exchange and correlation while building a functional, it is possible to obtain independently a large range of values for these parameters without any relation with the underlying real values. Therefore, it is concluded that the choice of a functional after a benchmark, especially using user-defined functionals, should be carried out with great care to avoid such effects.

KEYWORDS
absorption wavelength, DFT, exchange-correlation functional, structural analysis, TD-DFT

1 | INTRODUCTION

When dealing with density functional theory (DFT) computations, the functional that yields the energy from the electron density is a critical parameter.[1–3] Indeed, as no closed-form of this exact functional is currently known,[4] numerous approximated functionals have been built to approach the exact one as accurately as possible.[5] The construction of the functionals is a tough task owing to the fact that no systematic way to improve a functional does exist, even if the analytical form of the functional leads to a classification (LDA, GGA, meta-GGA, hybrid, and so forth) along which the quality of the approximation roughly increases.[6] The building of functionals is often a compromise between the inclusion of as many physical constraints as possible and a fit on large experimental data sets.[7] Therefore, the accuracy of approximated functionals is assessed by benchmarks that focus generally on the computation of some properties: among others, energetic, structural and spectroscopic quantities.[8–10] When a study includes both computational and experimental components, it is often, owing to the good accuracy/computation time ratio, DFT-based methods that are used. The choice of the functional is often assessed with some experimental data such as spectroscopic measurements, and used thereafter to compute other properties.

This study aims to focus on the limits that this approach encounters when applied to different properties. In this article, the case of two different flavonols (morin and quercetin, Figure 1) will be highlighted. Indeed, these naturally occurring molecules have been studied for several decades in our group, and possess interesting characteristics for this study.[11–13]

Like in biphenyl, the dihedral angle (C3—C2—C1′—C2′) between the chromone moiety and the phenyl ring of flavonols is an important structural parameter whose value results from two antagonistic effects: electronic delocalization on the entire molecule and steric hindrance. The value of this angle also varies with the physical state (gas, solid or in solution) of the molecule and can influence physicochemical

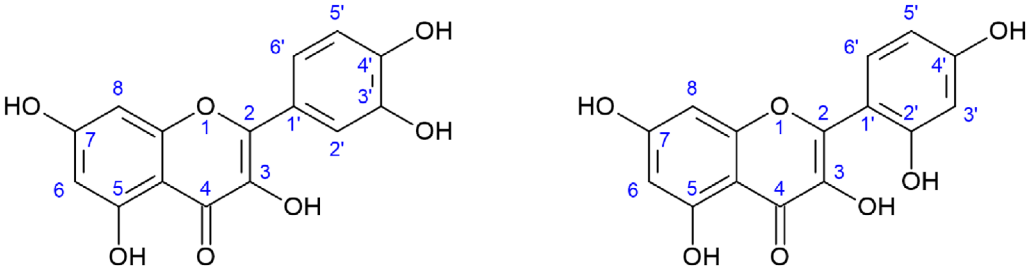

FIGURE 1 Structures of quercetin (left) and morin (right); along with the atomic numbering that is used throughout the article.

properties, for instance its solubility; this fact has been studied earlier.[14–16] The electronic absorption spectrum of flavonoids is characterized by two intense bands in the ultraviolet region whose positions are sensitive to the molecular environment. Because of this sensitivity, the wavelength corresponding to the lowest energy transition (called band I) is used to study the reactivity of flavonols and proceed to structural analyses.[17–19] These two properties should be related to each other, for the electron density transfer during the lowest energy electronic transition occurs mainly from the phenyl ring to the chromone moiety (see later for the justification of this assertion). Therefore, this article reports a comprehensive analysis of the variation of few selected parameters (including the dihedral angle and the lowest energy absorption wavelength) describing morin and quercetin along with the modification of the functional used. The computational section details the building of the used functionals, which originate from two widespread families.

2 | COMPUTATIONAL DETAILS

The DFT-based computations were carried out using the Gaussian 16 suite of programs.[20] The basis set used to describe the wave functions is 6–311+G(d,p),[21] which proved to be sufficient to converge the structural and spectroscopic properties (for instance References [18,19]). To avoid depending too heavily on this choice, part of the computations were carried simultaneously carried out with the Dunning triple-zeta basis set,[22] and no significant differences were observed.

Two widely used families of functionals were selected: BLYP[23–25] and PBE.[26] The objective of the study being to capture the effect of the variation of exchange and correlation contribution that can be adjusted in this software by using IOp keywords (specifically, 3/76, 3/77 and 3/78 were used, see Supporting Information for a sample input).

Using the nomenclature of the inputs used by the Gaussian software, a user-defined functional is written:

$$E_{xc} = P_2 E_X^{HF} + P_1\left(P_4 E_X^{Slater} + P_3 \Delta E_X^{nonlocal}\right) + P_6 E_c^{local} + P_5 \Delta E_c^{nonlocal},$$

where the six P_i parameters can be individually chosen. These choices define the hybridization of the functional (balance between P_1 and P_2), the ratio of non-local vs. local exchange (P_3 and P_4) and the same ratio for correlation energies (P_5 and P_6). For each family of functionals, these values were varied by increments of 5%.

The first set of functionals (set 1 in the following) was built to describe the simultaneous variations of the hybridization ratio and the amount of correlation energy. This debatable choice has been made in order to include in the comparison for the PBE family the GGA PBE, the global hybrid PBE0[27] and a Hartree-Fock like method. It was implemented using the following constraints:

$$P_1 + P_2 = 1.00, \quad (1)$$

$$P_3 = P_4 = 1.00, \quad (2)$$

$$P_5 = P_6. \quad (3)$$

Then, P_1 and P_5 were independently varied from 0.00 to 1.00 using an increment of 0.05 using PBE exchange and correlation contributions as non-local energies for the PBE family, and B88 exchange and LYP correlation contributions as non-local energies for the BLYP family. This leads to a total of 441 functionals for each family. Using this way to build the functionals, the popular B3LYP functional does not appear in this set. It should be noted that, for technical reasons linked to the used software, it was impossible to set $P_5 = P_6 = 0.0000$ (these settings were ignored). Thus, in these cases, we set instead $P_5 = P_6 = 0.0001$, a difference that is assumed to be negligible.

The second set of functional (set 2 in the following) was built to take into account two shortcomings from the previous one: to avoid removing the correlation energy (and instead to shift from local to non-local contributions), and to include B3LYP in the study. Therefore, the simultaneous variations of the non-local vs. local ratio were studied, and implemented using the following constraints:

$$P_2 = 0.25\,(\text{PBE})\ \text{or}\ 0.20\,(\text{BLYP}), \quad (4)$$

$$P_1 = P_6 = 1.00, \quad (5)$$

$$P_4 = 1.00 - P_2. \quad (6)$$

Then, P_3 and P_5 were independently varied from 0.00 to 1.00 using an increment of 0.05, and P_3 was scaled by P_4, leading to another set of 441 functionals for each family.

Once these sets of functional generated, the structure of the two molecules chosen in this study were optimized with each of them for a first part of the computations. In these cases, a vibrational analysis

was processed to check the validity of the minimum energy structure (no imaginary frequency was obtained). In a second part, computations are carried out on the structure obtained from PBE0. The difference between these computations is explicit in the text by referring to them as carried on "optimized" geometries and "reference" geometries, respectively.

All the computations were carried out in the vacuum.

The vibrational analyses were carried out in the harmonic approximation. For the computations of vertical excitations, the time-dependent formalism of DFT (TD-DFT) was used in the linear response approximation. The 50 lowest-lying excited states have been computed to ensure a good convergence of the lowest ones.

It is remarkable that the results obtained with the PBE and the B3LYP family are qualitatively the same, with only small quantitative differences. Thus, in the following, all the results are discussed, but the figures include only the results for the PBE family. The full set of results is reported in Supporting Information.

3 | RESULTS AND DISCUSSIONS

Quercetin and morin were fully optimized with the functionals included in the set 1, and the lowest energy transition was computed. The results are depicted for the PBE family on the Figure 2 (the same graphical depictions have been made for BLYP family and are reported in Figure S1). The results are in line with experimental values measured in the methanol from our previous studies (372 nm [3.33 eV] for quercetin and 354 nm [3.50 eV] for morin). It should be recalled that the main objective of this study is not the good reproduction of these values, an inclusion of the solvent would then be required, but the study of the effect of the functional on it. Nevertheless, it is reassuring that the computed values are in the same spectral domain as the experimental ones.

First, the four depictions are very similar from each other. The fact that PBE and BLYP families yield similar results is not surprising; only small quantitative differences are obtained. The similarity between quercetin and morin is more intriguing, since previous studies reported significant structural differences that are presented thereafter. More in details, the value of P_5 (percentage of correlation in the functional) does not influence the transition energy nor its oscillator strength. On the opposite, a large effect of the value of P_2 is observed, in line with the fact that Hartree-Fock exchange localizes the electron density more that pure DFT methods, implying the need of a larger energy to reorganize it. A statistical analysis was performed on these data to confirm this qualitative approach (the data is gathered in Table S1 and depicted on Figure 3).

In the case of the PBE family for quercetin (similar analyses yield analogous results for morin and for the BLYP family), when the Hartree-Fock exchange proportion (P_2) varies, the standard deviation of the transition energy ranges from 0.007 to 0.020 eV, while when the amount of correlation energy (P_5) varies, the standard deviation ranges from 0.579 to 0.602 eV. This analysis confirms the dependency of the studied transition energy to the proportion of HF exchange, and its non-dependency to the amount of correlation energy.

For both molecules, the studied transition involves the Highest Occupied (HOMO) to Lowest Unoccupied Molecular Orbital (LUMO) excitation (for more than 95%) for each functional. A typical example of the orbital pairs is depicted on the Figure 4 for quercetin and morin.

The general features of the electron transfer are the same in both cases. Upon transition, the electron density is lowered on the phenyl ring (especially on one of the hydroxyl [3′-OH in the case of quercetin and 2′-OH in the case of morin]) and the 3-OH group, and increased on the chromone part (more specifically the oxygen atoms [both the O1 and the O4]). As stated in the introduction, the electron transfer occurs via the inter-ring bond and could imply a significant role for the dihedral angle between the two molecular parts as its increase would lead to a decrease of the conjugation overall the molecules.

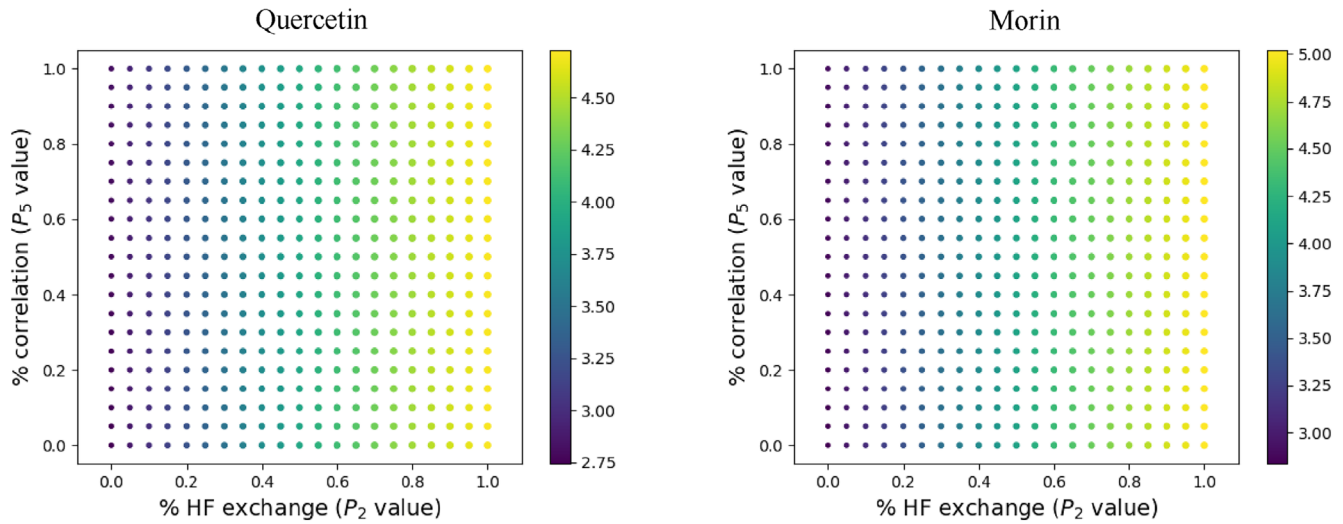

FIGURE 2 Lowest energy electronic transition computed for quercetin (left) and morin (right) using the set 1 of functionals for the PBE family. The transition energy (in eV) is given by the colorbar, the oscillator strength is indicated by the surface of the point.

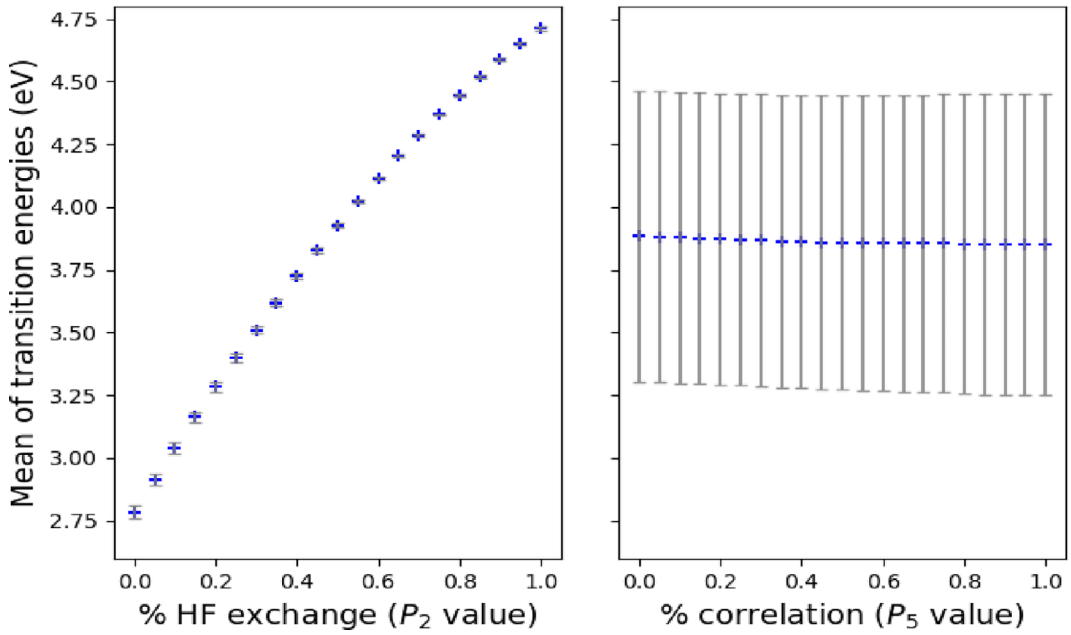

FIGURE 3 Mean of the computed lowest energy electronic transition (eV) (blue +) and the 1-σ interval (gray line, where σ is the standard deviation) when the P_2 value varies with P_5 value kept constant (left) and when the P_5 value varies with P_2 value kept constant (right) for quercetin using set 1 of functionals build within the PBE family.

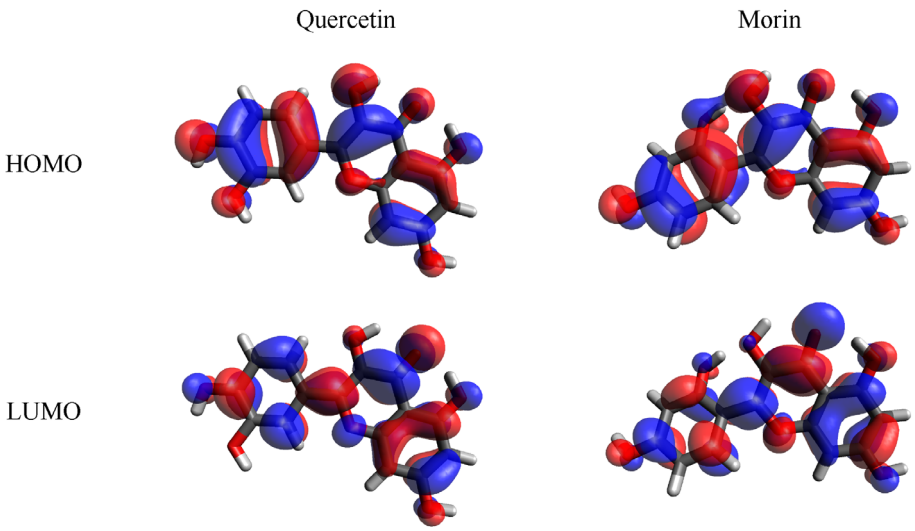

FIGURE 4 Shape of the HOMO and LUMO computed at the PBE0 level for quercetin (left) and morin (right).

Thus, the evolution of this angle has been computed for both molecules using the functionals included in set 1, and the 2D maps are reported on the Figure 5 for both molecules for the PBE family (BLYP family results are depicted on Figure S2 and do not differ significantly).

First, the difference between quercetin and morin that justified the study of these two molecules is obvious here: the quercetin molecule is planar for numerous functionals, especially those with the most chemical significance (P_5 not too far from 1, that means an inclusion of non-local correlation), whereas morin is twisted in all cases. To avoid any optimization trap in a planar local minimum, the starting structure for all molecules has been twisted (dihedral angle around 20°). A result from this analysis is stunning, especially in the case of quercetin: the variation of the dihedral angle occurs mainly with the P_5 parameter, that means in a direction orthogonal to the one that drives the variation of the energy of the electronic transition. The trend is less pronounced than for the transition energy, especially in the case of morin where the range in which the dihedral angles evolve is smaller than in quercetin (29.0°–38.1° for morin, 0.0°–17.9° for quercetin). To give more evidence, the range in which the means of the dihedral angle computed for each molecule are gathered in Table 1 and depicted, in the case of quercetin, on Figure 6 (full table [Table S2] and depiction [Figure S3]). With these values, the larger influence of P_5 versus P_2 appears clearly, that emphasizes the larger influence of the correlation amount compared to the HF proportion.

Remarkably, the qualitative results for the BLYP family reported in SI are in agreement, but the quantitative values are even more

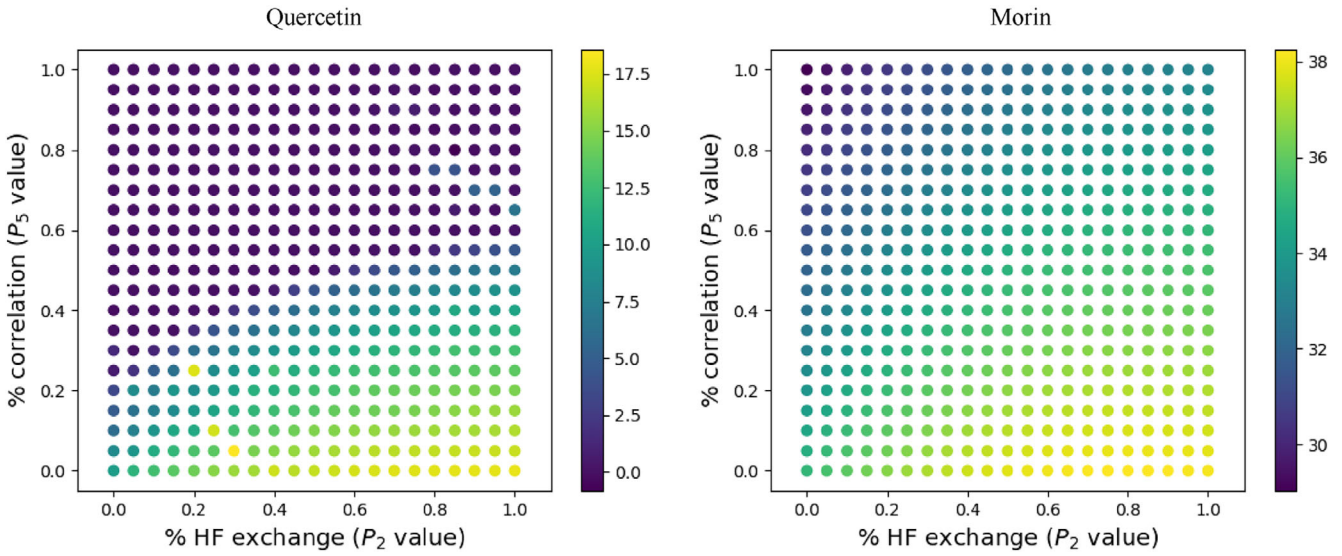

FIGURE 5 Dihedral angle computed for quercetin and morin using the set 1 of functionals for the PBE family. The dihedral angle (in °) is given by the colorbar.

TABLE 1 Minimal and maximal values of the mean of the computed dihedral angle (°) according to the considered variation (either P_2 or P_5) for quercetin and morin using set 1 of functionals build within the PBE family.

	Quercetin		Morin	
	Min. value	Max. value	Min. value	Max. value
P_2 varies, P_5 fixed	1.6	7.5	32.0	35.7
P_2 fixed, P_5 varies	0.0	16.0	31.8	37.4

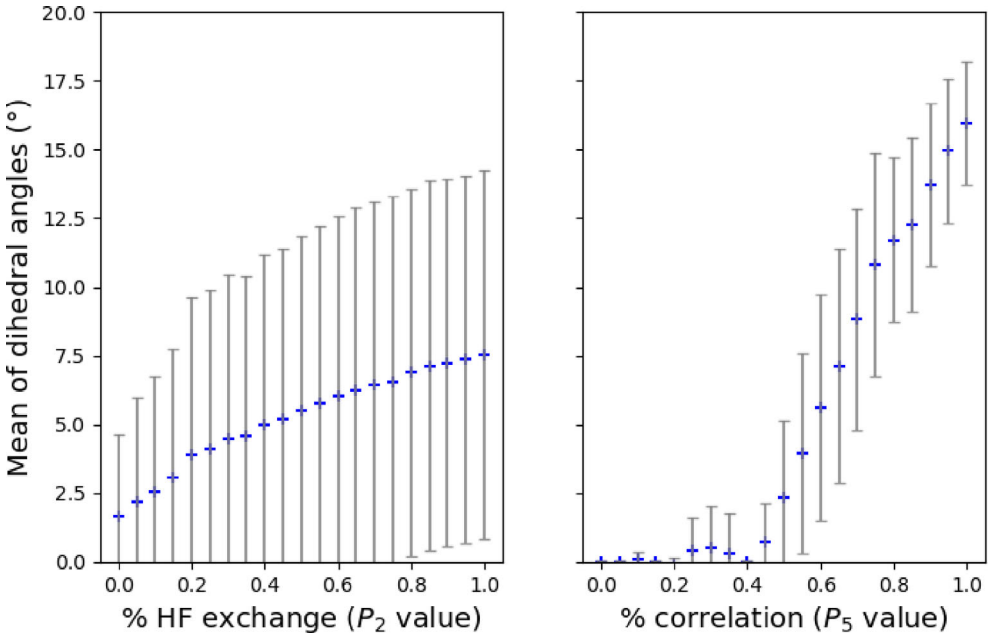

FIGURE 6 Mean of the computed dihedral angles (°) (blue +) and the 1-σ interval (gray line, where σ is the standard deviation) when the P_2 value varies with P_5 value kept constant (left) and when the P_5 value varies with P_2 value kept constant right) for quercetin using set 1 of functionals build within the PBE family.

convincing. To analyze more accurately this change, the inter-ring C2—C1′ bond has been studied as it is another geometrical parameter linked to the dihedral angle: if the dihedral angle is close to 0°, the larger conjugation between both rings could lead to a shortening of the C2—C1′ bond as the consequence of the increased bond order. The general trend is recovered (for a fixed value of P_2, the smaller the angle, the shorter the C2—C1′ bond), but any attempt to be more accurate fails (results depicted on Figure 5). Indeed, the changes are smoother in the case of the bond lengths, and the variation is less convincing for a fixed value of P_5: whereas there is still an opposite variation of the dihedral angle and of the C—C bond, the last one varies also when the angle does not change, that means that the bond

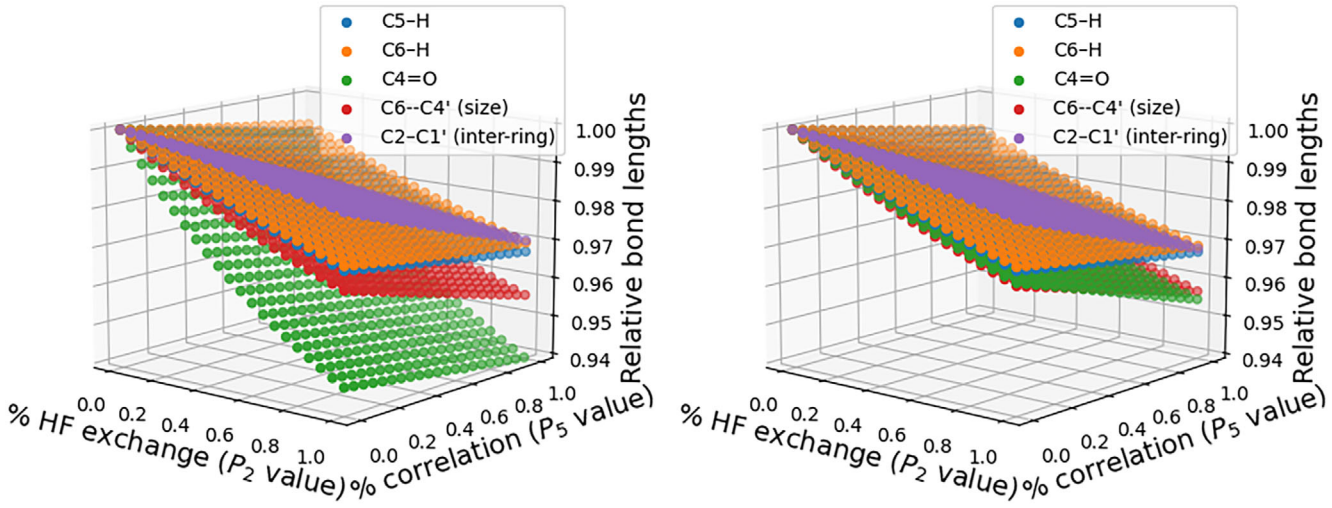

FIGURE 7 Relative values of some selected inter-atom distances computed for quercetin (left) and morin (right) using the set 1 of functionals for the PBE family.

variation also has other origins. Thus, other bonds chosen to be independent of the dihedral angle have been studied. Four of them have been selected: two C—H bonds (C5′—H and C6′—H) that should be only scarcely altered by the rotation of the angle, the C4═O double bond, and a distance directly linked to the length of the molecule (C6—C4′). The variations for these four bond lengths are depicted on Figure 7 in the case of the PBE family along with the inter-ring bond (the data for the BLYP family are similar and reported on Figure S4). To make the comparison easier, the relative values of the bond lengths compared to the longest cases ($P_2 = P_5 = 0$ in each case) are overlapped instead of the effective values and the z-axis is the same for all graphs.

Remarkably, the trend is the same for four of them (C5′—H, C6′—H, C4═O and C6—C4′): P_5 effect is quite small when compared to P_2 effect, contrarily to the last one (inter-ring bond) where the magnitude of both effects is similar. This difference is striking on the figures: the quasi-plane that represents the evolution of the inter-ring bond has an orientation that differs significantly form the other four. The parameters related to the backbone of the molecules vary similarly in the two studied molecules, whereas the C4═O evolution is different. The larger evolution computed in the case of quercetin could be linked to the larger flexibility of this molecule, that is illustrated by the magnitude of the dihedral angle evolution (that could be interpreted as a consequence of the hydrogen bonds network that makes the morin more rigid).

Thus, the evolution of the inter-ring bond could be attributed to at least two independent parameters: the general evolution of the bond lengths in the molecules (P_2 effect mainly) and the change in the dihedral angle evoked earlier (P_5 effect). The combination of these two parameters (or more) would lead to a complex evolution that cannot be easily described as the interference between these parameters is unknown.

Once established that the bond lengths bear significant changes on the set 1 of functionals, it is logical to wonder if this influence is recoverable while studying the vibrations of the molecules. The vibration modes involve a large number of mechanical couplings between vibrators throughout the molecule, therefore a precise study of all of them would be though and of little interest. Notably, the inter-ring stretching, which is of particular interest in this study, is not a pure mode but has a potential energy distributed over many modes. The vibration mode including the C4═O stretching is easily localized, in between the O/C—H stretching and the normal modes of phenyl ring. In both molecules, this mode is numbered 80 (with the numbering starting with the lowest wavenumber values). The changes in wavenumbers of this mode with both P_2 and P_5 parameters are depicted on Figure 8 in the case of the PBE family (the full results are gathered on Figure S5).

Once again, the results does not differ significantly depending on the molecule or the family of functionals used. The result obtained is reassuring, the variation of the vibrational mode energy being correlated: the shorter the bond is (large P_2 and P_5 values), the higher the vibration energy is. This expected result comforts us in the idea that the geometrical features, including the harmonic vibrational frequencies bears a dependency on the functional used that is more complex that the dihedral angle or the lowest electron transition energy. It should be remarked that a maximum of the IR intensities is computed close to $P_2 = 0.2$, close to the values used for the widely used functionals emerging from these families (PBE0 and B3LYP).

Then, to further study the effect of the functional on the intertwinement between electronic transition and geometry, the effect of the optimization of the geometry was checked. As explained in the computational details section, the geometry of the molecules optimized at the PBE0 level was used to compute the lowest electronic absorption energy using the set 1 of functionals with the PBE family. Indeed, the previous results about the closeness of the results computed for the BLYP and the PBE family were convincing enough to focus the computations only on one family. The result of this analysis is depicted on Figure S6. The main result is the lack of qualitative difference between the optimized case and the use of a reference geometry. A small quantitative difference is obtained, the computed values

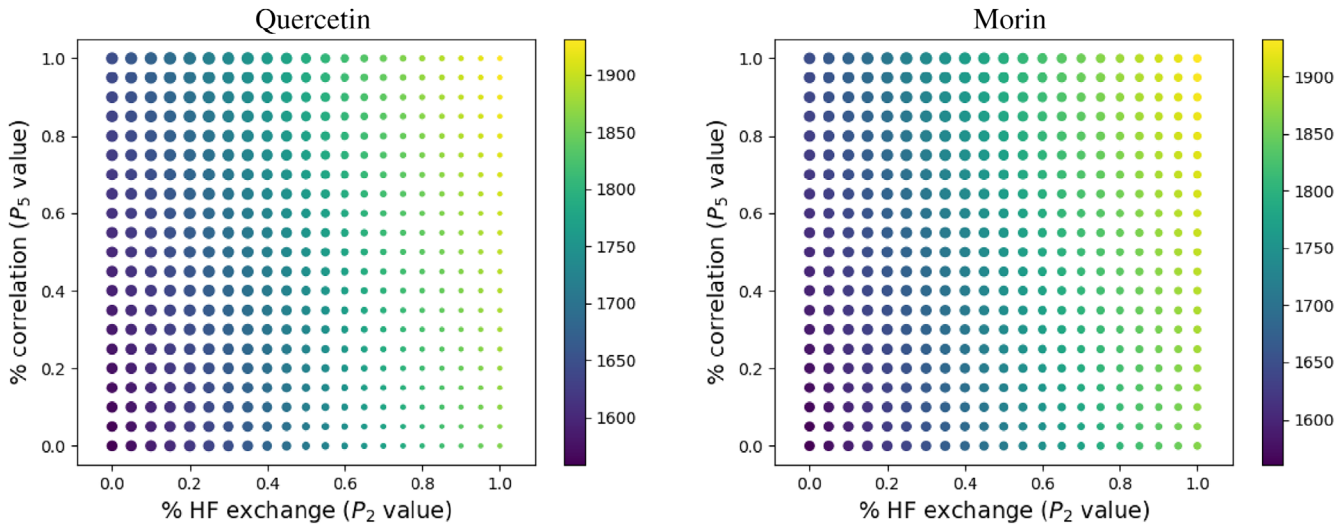

FIGURE 8 Mode 80 vibration energy computed for quercetin (left) and morin (right) using the set 1 of functionals for the PBE family. The vibration energy (in cm^{-1}) is given by the colorbar, the infrared intensity is indicated by the surface of the point.

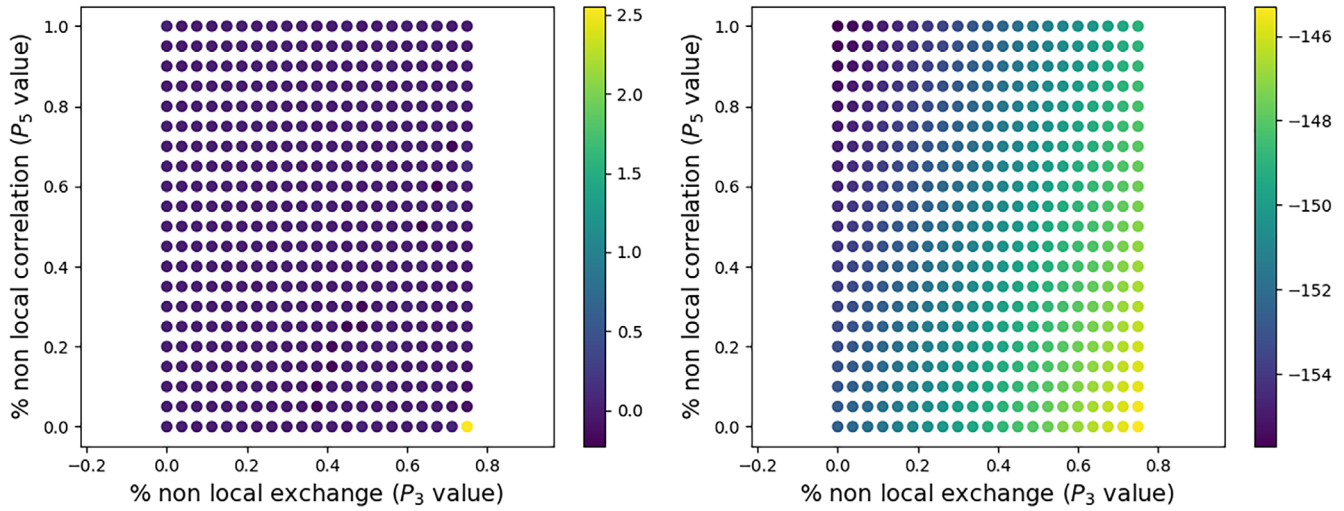

FIGURE 9 Dihedral angle computed for quercetin (left) and morin (right) using the set 2 of functionals for the PBE family. The dihedral angle (in °) is given by the colorbar. Be aware that the scale is different from previous figures.

being more centered: for instance, in the case of quercetin, the scales ranges in the case from 3.0 to 4.4 eV, while it was from 2.8 to 4.5 eV using optimized geometries. Nevertheless, once again, the transition energy value appears to be driven only by the P_2 value, and this trend appears to be independent of the geometry used. In this case, the surprising fact is not the dependency on the value of P_2 that is well-established, but the independency on the value of P_5 that indicates a tiny influence of the functional used for the optimization.

Last, a glimpse on the effect of the balance between local and non-local contribution to the exchange and correlation energies was obtained. The most significant results are depicted on Figures S7–S9: the variation of the lowest absorption wavelength (Figure S7) and the dihedral angle (Figure 9 for the PBE family and Figure S8 for the whole set) was studied with respect to the P_3 and P_5 values, using the same data set as previously. Generally speaking, the variations are quite small, so the trend are difficult to explain. The lowest electronic transition energy is shifted from less than 0.12 eV in the case of morin and 0.07 eV in the case of quercetin on the whole data set. In both cases, a small percentage of non-local correlation (P_5) and a large percentage of non-local exchange (P_3) lead to higher transition energies. This association is odd and is not often used in current density functional approximations (as illustrated by the composition of PBE0 and B3LYP). The dihedral angle (Figure 9) follows the same trends, with a change below 9° in the case of morin and 7° in the case of quercetin. Larger values were obtained for the same case as for the electronic transition, with small values for P_5 and large for P_3.

The use of a reference geometry (Figure S9) or of an optimized geometry to compute the electronic transition energy was once again

quite small. The main conclusion to be drawn from the use of the set 2 is that the exact composition (local vs. non-local) of the functional used in this study has a negligible effect with respect to the effect of the proportion of true exchange or the amount of non-local correlation illustrated with set 1.

4 | CONCLUSIONS

A large number of functionals was built from the PBE and BLYP families by varying several internal parameters and it has been used to compute several spectroscopic and structural properties for two small molecules. A focus has been put on two key quantities (a dihedral angle and an electronic absorption wavelength) to understand if a clear link was observed between the functional used and the computed quantities. From a physical point of view, these two quantities are closely intertwined: rotation around the inter-ring bond influences the flatness of the molecule and the charge transfer observed in the lowest energy transition occurs via this bond.

To be comprehensive, it was shown that:

1. the absorption wavelength is mostly driven by the proportion of Hartree-Fock exchange;
2. the inter-ring angle is mostly driven by the amount of correlation;
3. the variations of bonds lengths are more complex. Most of them are mostly driven by the Hartree-Fock exchange, but those correlated to the inter-ring angle are also affected by the amount of correlation;
4. the local or non-local nature of the correlation has a role significantly smaller than the proportion of Hartree-Fock exchange or the amount of correlation.

From the calculations, it can be concluded that, at least in the studied molecules, a specific value can be assigned independently, in a reasonable range, to the two selected quantities by the choice of a specific functional. This behavior is expected to be reproduced for other classes of molecules as the studied molecules are quite simple and do not present features that will make them stand out of others. Thus, it confirms in a remarkable way that the methodology that consists in choosing a density functional approximation on the basis of the good reproduction of one measurable quantity (for instance an electronic transition) to deduce another quantity (for instance an angle value) should be used carefully to avoid this phenomenon. Therefore, sticking to functionals that have been validated by independent works instead to proceed to large benchmarks, especially with ad hoc-built functionals, is certainly a better practice.

ACKNOWLEDGMENTS

The authors would like to acknowledge the High Performance Computing Center of the University of Lille for supporting this work by providing access to computing resources. First computations on this subject have been carried by Anaëlle Raoumbe Djendja to whom the authors are very grateful.

DATA AVAILABILITY STATEMENT

The data that support the findings of this study are available from the corresponding author upon reasonable request.

ORCID

Aurélien Moncomble https://orcid.org/0000-0002-4362-269X
Jean-Paul Cornard https://orcid.org/0000-0003-1996-0450

REFERENCES

[1] P. Hohenberg, W. Kohn, *Phys. Rev.* **1964**, *136*, B864.
[2] J. P. Perdew, A. Ruzsinszky, *Int. J. Quantum Chem.* **2010**, *110*, 2801.
[3] A. D. Becke, *J. Chem. Phys.* **2014**, *140*, 18A301.
[4] E. H. Lieb, *Int. J. Quantum Chem.* **1983**, *24*, 243.
[5] J. Toulouse, in *Density Functional Theory: Modeling, Mathematical Analysis, Computational Methods, and Applications* (Eds: E. Cancès, G. Friesecke), Springer International Publishing, Cham **2023**, 1. https://doi.org/10.1007/978-3-031-22340-2_1
[6] J. P. Perdew, K. Schmidt, *AIP Conf. Proc.* **2001**, *577*, 1.
[7] K. Burke, in *Lecture Notes in Physics*, Vol. 706 (Eds: M. A. L. Marques, C. A. Ullrich, F. Nogueira, A. Rubio, K. Burke, E. K. U. Gross, R. Beig, W. Beiglböck, W. Domcke, B.-G. Englert, U. Frisch, P. Hänggi, G. Hasinger, K. Hepp, W. Hillebrandt, D. Imboden, R. L. Jaffe, R. Lipowsky, H. V. Löhneysen, I. Ojima, D. Sornette, S. Theisen, W. Weise, J. Wess, J. Zittartz), Springer, Berlin Heidelberg **2006**, p. 181.
[8] N. Kosar, K. Ayub, M. A. Gilani, S. Muhammad, T. Mahmood, *ACS Omega* **2022**, *7*, 20800.
[9] C. Zhao, R. Wu, S. Zhang, X. Hong, *J. Phys. Chem. A* **2023**, *127*, 6791.
[10] A. D. Laurent, D. Jacquemin, *Int. J. Quantum Chem.* **2013**, *113*, 2019.
[11] A. Moncomble, C. Falantin, J.-P. Cornard, *J. Phys. Chem. B* **2018**, *122*, 8943.
[12] A. Moncomble, J.-P. Cornard, *RSC Adv.* **2014**, *4*, 29050.
[13] A. Moncomble, D. J. Thaviligadu, A. R. Djendja, J.-P. Cornard, *New J. Chem.* **2018**, *42*, 7691.
[14] S. Aparicio, *Int. J. Mol. Sci.* **2010**, *11*, 2017.
[15] G. Lewin, A. Maciuk, A. Moncomble, J.-P. Cornard, *J. Nat. Prod.* **2013**, *76*, 8.
[16] H. M. Ali, I. H. Ali, *Med. Chem. Res.* **2019**, *28*, 2262.
[17] T. J. Mabry, K. R. Markham, M. B. Thomas, in *The Systematic Identification of Flavonoids* (Eds: T. J. Mabry, K. R. Markham, M. B. Thomas), Springer, Berlin, Heidelberg **1970**, p. 41. https://doi.org/10.1007/978-3-642-88458-0_5
[18] L. Labarrière, A. Moncomble, J.-P. Cornard, *RSC Adv.* **2020**, *10*, 35017.
[19] D. J. Thaviligadu, L. Labarrière, A. Moncomble, J.-P. Cornard, *Spectrochim. Acta A* **2020**, *225*, 117492.
[20] M. J. Frisch, G. W. Trucks, H. B. Schlegel, G. E. Scuseria, M. A. Robb, J. R. Cheeseman, G. Scalmani, V. Barone, B. Mennucci, G. A. Petersson, H. Nakatsuji, M. Caricato, X. Li, H. P. Hratchian, A. F. Izmaylov, J. Bloino, G. Zheng, J. L. Sonnenberg, M. Hada, M. Ehara, K. Toyota, R. Fukuda, J. Hasegawa, M. Ishida, T. Nakajima, Y. Honda, O. Kitao, H. Nakai, T. Vreven, J. A. Montgomery Jr., J. E. Peralta, F. Ogliaro, M. J. Bearpark, J. Heyd, E. N. Brothers, K. N. Kudin, V. N. Staroverov, R. Kobayashi, J. Normand, K. Raghavachari, A. P. Rendell, J. C. Burant, S. S. Iyengar, J. Tomasi, M. Cossi, N. Rega, N. J. Millam, M. Klene, J. E. Knox, J. B. Cross, V. Bakken, C. Adamo, J. Jaramillo, R. Gomperts, R. E. Stratmann, O. Yazyev, A. J. Austin, R. Cammi, C. Pomelli, J. W. Ochterski, R. L. Martin, K. Morokuma, V. G. Zakrzewski, G. A. Voth, P. Salvador, J. J. Dannenberg, S. Dapprich, A. D. Daniels, Ö. Farkas, J. B. Foresman, J. V. Ortiz, J. Cioslowski, D. J. Fox, Gaussian 16 A.03. **2016**.

[21] R. Krishnan, J. S. Binkley, R. Seeger, J. A. Pople, *J. Chem. Phys.* **1980**, *72*, 650.
[22] R. A. Kendall, T. H. Dunning, R. J. Harrison, *J. Chem. Phys.* **1992**, *96*, 6796.
[23] A. D. Becke, *Phys. Rev. A* **1988**, *38*, 3098.
[24] C. Lee, W. Yang, R. G. Parr, *Phys. Rev. B* **1988**, *37*, 785.
[25] S. H. Vosko, L. Wilk, M. Nusair, *Can. J. Phys.* **1980**, *58*, 1200.
[26] J. P. Perdew, K. Burke, M. Ernzerhof, *Phys. Rev. Lett.* **1996**, *77*, 3865.
[27] C. Adamo, V. Barone, *J. Chem. Phys.* **1999**, *110*, 6158.

SUPPORTING INFORMATION

Additional supporting information can be found online in the Supporting Information section at the end of this article.

How to cite this article: A. Moncomble, J.-P. Cornard, *J. Comput. Chem.* **2024**, 1. https://doi.org/10.1002/jcc.27382